AIP | Journal of Applied Physics

Concurrent operational modes and enhanced current sensitivity in heterostructure of magnetoelectric ring and piezoelectric transformer

Shengyao Zhang, Chung Ming Leung, Wei Kuang, Siu Wing Or, and S. L. Ho

Citation: J. Appl. Phys. **113**, 17C733 (2013); doi: 10.1063/1.4801390
View online: http://dx.doi.org/10.1063/1.4801390
View Table of Contents: http://jap.aip.org/resource/1/JAPIAU/v113/i17
Published by the AIP Publishing LLC.

JOURNAL OF APPLIED PHYSICS **113**, 17C733 (2013)

Concurrent operational modes and enhanced current sensitivity in heterostructure of magnetoelectric ring and piezoelectric transformer

Shengyao Zhang, Chung Ming Leung, Wei Kuang, Siu Wing Or,[a] and S. L. Ho
Department of Electrical Engineering, The Hong Kong Polytechnic University, Hung Hom, Kowloon, Hong Kong

(Presented 17 January 2013; received 5 November 2012; accepted 4 February 2013; published online 15 April 2013)

A heterostructure possessing two concurrent operational modes: current sensing (CS) mode and current transduction (CT) mode and an enhanced current sensitivity associated with the CT mode is proposed by combining a magnetoelectric ring (MER) with a piezoelectric transformer (PET). The MER is a ring-shaped magnetoelectric laminate having an axially polarized Pb(Zr, Ti)O_3 (PZT) piezoelectric ceramic ring sandwiched between two circumferentially magnetized, inter-magnetically biased $Tb_{0.3}Dy_{0.7}Fe_{1.92}$ (Terfenol-D) short-fiber/NdFeB magnet/epoxy three-phase magnetostrictive composite rings, while the PET is a Rosen-type PZT piezoelectric ceramic transformer. The current sensitivity (S_I) and magnetoelectric voltage coefficient (α_V) of the heterostructure in the two operational modes are evaluated theoretically and experimentally. The CS mode provides a large S_I of ~10 mV/A over a flat frequency range of 10 Hz−40 kHz with a high resonance S_I of 157 mV/A at 62 kHz. The CT mode gives a 6.4-times enhancement in resonance S_I, reaching 1000 mV/A at 62 kHz, as a result of the amplified vortex magnetoelectric effect caused by the vortex magnetoelectric effect in the MER, the matching of the resonance frequencies between the MER and the PET, and the resonance voltage step-up effect in the PET.
 [http://dx.doi.org/10.1063/1.4801390]

Magnetoelectric laminates based on magnetostrictive and piezoelectric materials have emerged as an important type of magnetoelectric materials for passive magnetic field sensors and magnetoelectric transducers.[1,2] The research work in the past decade has resulted in various interesting laminates for detection of magnetic fields of constant direction, including plate-shaped laminates with longitudinal or transverse magnetization and polarization,[1] disk-shaped laminates with radial or axial magnetization and polarization,[2] etc. Because of the unidirectional magnetic field detection nature, these laminates can only get access to a small path of vortex magnetic fields governed by Ampère's law in current-carrying electric cables or conductors. This deficiency significantly limits the detection accuracy and application prospects of the laminates for electric current sensors.

To enable vortex magnetic field detection and electric current sensing at high frequencies, we have recently developed a ring-shaped magnetoelectric laminate (called magnetoelectric ring (MER)) featuring a high non-resonance current sensitivity (S_I) of 12.6 mV/A over a broad frequency range of 1 Hz–30 kHz and a large resonance S_I of 92.2 mV/A at 67 kHz by laminating an axially polarized Pb(Zr, Ti)O_3 (PZT) piezoelectric ceramic ring between two circumferentially magnetized, inter-magnetically biased $Tb_{0.3}Dy_{0.7}Fe_{1.92}$ (Terfenol-D) short-fiber/NdFeB magnet/epoxy three-phase magnetostrictive composite rings.[3] The evolution of magnetoelectricity has called for broadband general detection of magnetic fields and electric currents on the one hand and for narrowband precision detection on the other hand.[4] Hence, it is of great scientific and practical values if the non-resonance and resonance S_I of our developed MER can be utilized to configure a broadband sensing mode for general detection and a narrowband transduction mode for precision detection, both in concurrent operation.

In this paper, we report theoretically and experimentally the presence of two concurrent operational modes: namely, current sensing (CS) mode and current transduction (CT) mode as well as an enhanced S_I associated with the CT mode in a heterostructure formed by introducing a MER to a piezoelectric transformer (PET). The structure and working principle of the heterostructure are presented, together with the characteristics of the two concurrent operational modes.

Figure 1 shows the schematic diagram of the proposed heterostructure formed by connecting the output of a MER to the input of a PET. The MER is a ring-shaped magnetoelectric laminate having a CeramTec P8 PZT piezoelectric ceramic ring of outer radius (R_2) 12.5 mm, inner radius (R_1) 5 mm, thickness (t_p) 3 mm, and axial polarization (P) bonded between two self-prepared Terfenol-D short-fiber/NdFeB magnet/epoxy three-phase magnetostrictive composite rings of the same dimensions and with circumferential magnetization (M) and internal magnetic biasing using a conductive epoxy adhesive. Details of the fabrication of the MER and the magnetostrictive composite rings can be found elsewhere.[3,5] The PET is a Rosen-type PZT piezoelectric ceramic transformer of length ($l_1 + l_2$) 27 mm, width (w) 8 mm, and thickness (t) 1.8 mm in order to match its fundamental longitudinal resonance frequency with the fundamental radial resonance frequency of the MER for maximizing

[a]Author to whom correspondence should be addressed. Electronic mail: eeswor@polyu.edu.hk.

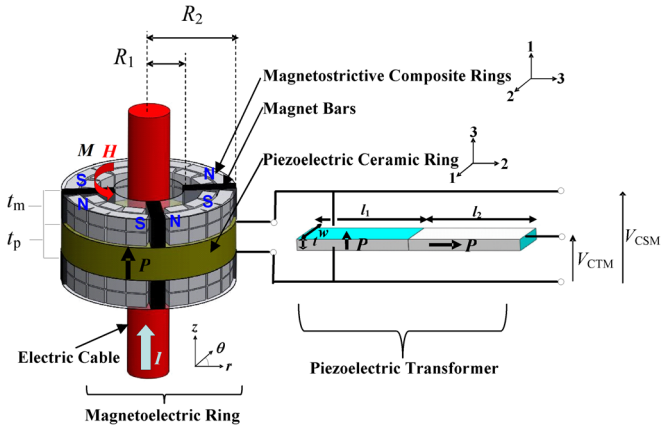

FIG. 1. Schematic diagram of the proposed MER–PET heterostructure. The arrows *M* and *P* denote the magnetization and polarization directions of the magnetostrictive composite rings and the piezoelectric ceramic ring, respectively. N and S indicate the north and south poles of the magnet bars.

the magnetoelectric energy conversion and amplification under resonance conditions.[6]

The MER–PET heterostructure in Fig. 1 has two concurrent operational modes: CS mode and CT mode. In the CS mode of operation, an ac electric current (I) flowing through an electric cable in the axial (or z-) direction induces an ac vortex magnetic field (H) along the length of the cable in accordance with Ampère's law.[7] Due to the nonuniform distribution of H over the volume of the MER, an average ac vortex magnetic field (H_{avg}) is detected by the MER which, in turn, causes the top and bottom magnetostrictive composite rings to produce radial (r) motions based on the magnetostrictive effect.[3] Because of the mechanical coupling, the induced magnetostrictive strains lead to stresses in the central piezoelectric ceramic ring, thereby producing an ac piezoelectric voltage (V_{CSM}) across the thickness of the piezoelectric ceramic ring based on the piezoelectric effect. This V_{CSM} corresponds to the magnetoelectric voltage output from an individual MER (V_{MER}), provided that the output impedance of the MER is much smaller than the input impedance of the PET. In the CT mode of operation, this V_{CSM} is further subject to the resonance voltage step-up effect in the PET. As the PET behaves essentially a narrowband voltage step-up transformer with a high voltage step-up ratio (A_V) around its fundamental longitudinal resonance,[6] and since the fundamental longitudinal resonance frequency of the PET is designated to match with the fundamental radial resonance frequency of the MER, a significantly enhanced ac electric voltage (V_{CTM}), which is the product of V_{CSM} and A_V, is achieved at the output of the PET at resonance. This is said to be the amplified vortex magnetoelectric effect caused by the vortex magnetoelectric effect in the MER, the matching of the resonance frequencies between the MER and the PET, and the resonance voltage step-up effect in the PET.

Theoretically, the magnetoelectric voltage coefficient of the MER ($\alpha_{V,MER} = dV_{MER}/dH_{avg}$) can be modeled using the constitutive piezomagnetic equations for the circumferentially magnetized magnetostrictive composite rings,[8] the constitutive piezoelectric equations for the axially polarized piezoelectric ceramic ring,[9] and the elastodynamic equation for radial vibrations[9] with stress-free and open-circuit boundary conditions. Details can be found elsewhere.[10] Using Ampère's law to correlate I and H_{avg} in an electric cable[7] and taking the product of dH_{avg}/dI and $\alpha_{V,MER}$, the current sensitivity of the MER ($S_{I,MER}$) can be expressed as

$$S_{I,\mathrm{MER}} = \frac{dV_{\mathrm{MER}}}{dH_{\mathrm{avg}}}\frac{dH_{\mathrm{avg}}}{dI} = \alpha_{V,\mathrm{MER}}\frac{1}{\pi(R_1+R_2)}. \quad (1)$$

For the PET, the voltage step-up ratio (A_V) can be modeled using an equivalent-circuit approach and expressed as follows:[11]

$$A_V = \left|\frac{R'' - j\frac{1}{\omega C''}}{R' + R'' + j\left(\omega L' - \frac{1}{\omega C'} - \frac{1}{\omega C''}\right)}\right|\frac{\phi}{\psi}, \quad (2)$$

where $R' = \frac{R_m}{\phi^2}$, $L' = \frac{m}{\phi^2}$, $C' = C_m\phi^2$; $R'' = \frac{R_L}{1+\omega^2 C_{02}^2 R_L^2}\frac{\psi^2}{\phi^2}$, $C'' = \frac{(1+\omega^2 C_{02}^2 R_L^2)\phi^2}{\omega^2 C_{02} R_L^2 \psi^2}$; $\phi = d_{31,t}W/s^E_{11,t}$ is the electromechanical energy conversion coefficient; $\psi = d_{33,t}Wt/s^E_{33,t}l_2$ is the mechanoelectric energy conversion coefficient; ω is the angular frequency; m, C_m, and R_m are the equivalent mechanical mass, compliance, and resistance, respectively; R_L is the load resistance; and $C_{02} = \varepsilon^T_{33,t}(1-k^2_{33,t})Wt/l_2$ is the clamped capacitance.

For the heterostructure, the current sensitivities of the CS mode ($S_{I,CSM}$) and the CT mode ($S_{I,CTM}$) can be expressed, respectively, as

$$S_{I,\mathrm{CSM}} \approx S_{I,\mathrm{MER}} \quad (3)$$

and

$$S_{I,\mathrm{CTM}} = S_{I,\mathrm{CSM}} \cdot A_V. \quad (4)$$

Figure 2(a) shows the frequency (f) dependence of the measured and calculated $S_{I,MER}$ and $\alpha_{V,MER}$ of the MER energized by an electric cable of 4 mm diameter at an applied I of 1 A peak. It is clear that the measured $S_{I,MER}$ and $\alpha_{V,MER}$ spectra agree well with the calculated ones based on Eq. (1). $S_{I,MER}$ and $\alpha_{V,MER}$ are measured to be ~11 mV/A and

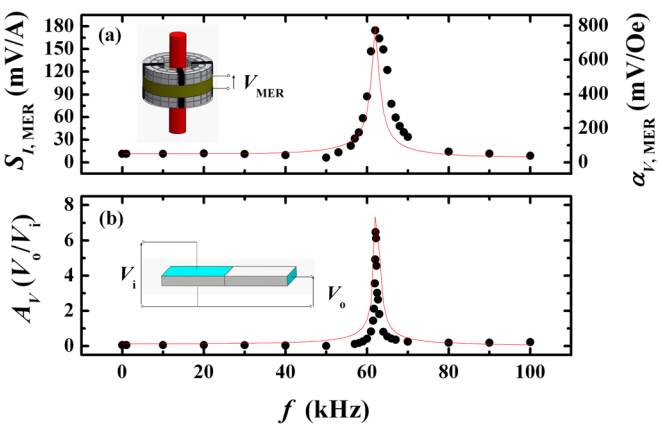

FIG. 2. Measured (symbol) and calculated (line) spectra of (a) $S_{I,MER}$ and $\alpha_{V,MER}$ of the MER and (b) A_V of the PET.

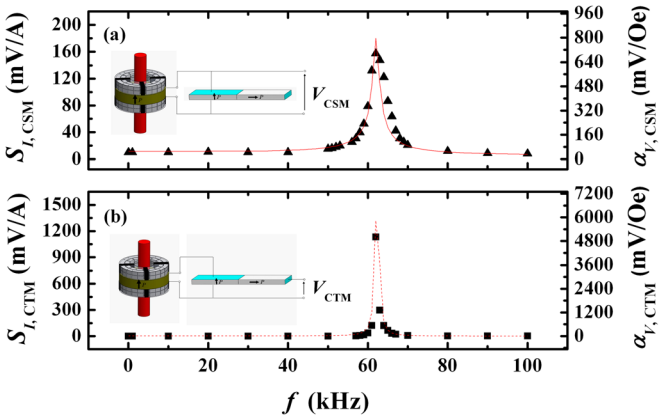

FIG. 3. Measured (symbols) and calculated (lines) spectra of (a) $S_{I,CSM}$ and $\alpha_{V,CSM}$ for the CS mode and (b) $S_{I,CTM}$ and $\alpha_{V,CTM}$ for the CT mode in the heterostructure.

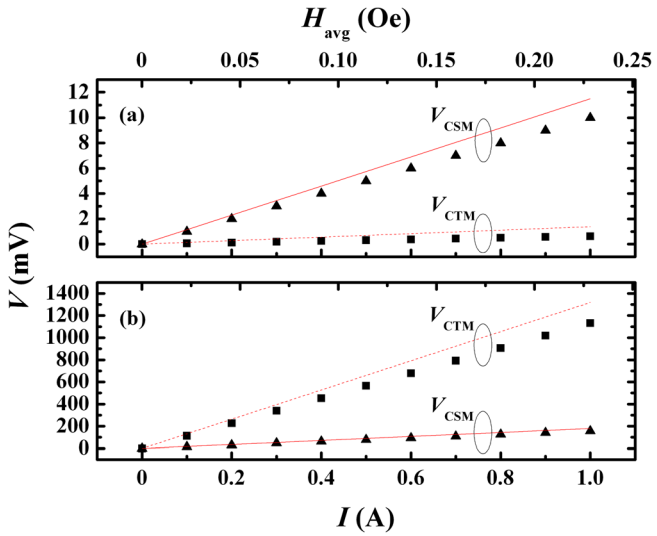

FIG. 4. Measured (symbols) and calculated (lines) V_{CSM} and V_{CTM} of the heterostructure as functions of applied I and its corresponding H_{avg} at (a) the non-resonance f of 10 Hz and (b) the resonance f of 62 kHz.

~48 mV/Oe, respectively, in the non-resonance f range up to 40 kHz. At 62 kHz, $S_{I,MER}$ and $\alpha_{V,MER}$ are greatly enhanced to 164 mV/A and 761 mV/Oe, respectively, because of the effect of the fundamental magnetoelectric radial resonance. Figure 2(b) plots the measured and calculated A_V of the PET in the same f range. The measured A_V is well predicted by Eq. (2). The highest A_V of 6.5 as measured at 62 kHz is the fundamental electromechanical longitudinal resonance of the PET.[11] The observations in Fig. 2 suggest that in addition to the broadband CS mode enabled by the MER for general detection in Fig. 2(a), a narrowband CT mode with enhanced resonance S_I and α_V can be created concurrently for precision detection by cascade operation of the MER and PET at 62 kHz.

Figure 3 shows the measured and calculated S_I spectra of the heterostructure in the CS and CT modes at an applied I of 1 A peak. The corresponding α_V spectra are also included for information. For the CS mode of operation in Fig. 3(a), $S_{I,CSM}$ remains essentially high and stable at ~10 mV/A in the broad f range of 10 Hz–40 kHz and attends a maximum value of 157 mV/A at 62 kHz. For the CT mode of operation in Fig. 3(b), $S_{I,CTM}$ exhibits a giant value of 1000 mV/A, also at 62 kHz, in comparison with ~0.6 mV/A at non-resonance frequencies. This resonance $S_{I,CTM}$ is even 6.4-times larger than the resonance $S_{I,CSM}$ of 157 mV/A in Fig. 3(a) and can be ascribed to the amplified vortex magnetoelectric effect caused by the vortex magnetoelectric effect in the MER, the matching of the resonance frequencies between the MER and the PET, and the resonance voltage step-up effect in the PET. The good agreement between the measured and calculated S_I spectra also confirms the validity of Eqs. (3) and (4).

Figure 4 plots the measured and calculated V_{CSM} and V_{CTM} of the heterostructure as functions of applied I and its corresponding H_{avg} at the non-resonance f of 10 Hz (Fig. 4(a)) and the resonance f of 62 kHz (Fig. 4(b)). It is seen that the measured V_{CSM} and V_{CTM} have good agreements with the calculated V_{CSM} and V_{CTM}, all demonstrating good linear responses to I and H_{avg}. From the slopes of the plots, the measured $S_{I,CSM}$ and $S_{I,CTM}$ are found to be ~10 mV/A and ~0.6 mV/A at 10 Hz, and 157 mV/A and 1000 mV/A at 62 kHz, respectively, being coincided with those observed from Fig. 3.

We have developed a MER–PET heterostructure with concurrent CS and CT modes of operation for broadband general detection and narrowband precision detection of vortex magnetic fields and hence electric currents governed by Ampère's law in electric cables or conductors, respectively. The theoretical and experimental evaluations of S_I and α_V of the heterostructure in the two concurrent operational modes have revealed a large S_I of ~10 mV/A over a flat frequency range of 10 Hz−40 kHz with a high resonance S_I of 157 mV/A at 62 kHz in the CS mode as well as a greatly enhanced resonance S_I of 1000 mV/A at 62 kHz in the CT mode as a result of the amplified vortex magnetoelectric effect caused by the vortex magnetoelectric effect in the MER, the matching of the resonance frequencies between the MER and the PET, and the resonance voltage step-up effect in the PET.

This work was supported by The Hong Kong Polytechnic University under Grant Nos. H-ZG76, 1-ZV7P, G-RPT2, and G-RPEP.

[1]M. Fiebig, J. Phys. D: Appl. Phys. **38**, R123 (2005).
[2]J. Ryu *et al.*, Jpn. J. Appl. Phys., Part 1 **40**, 4948 (2001).
[3]C. M. Leung *et al.*, J. Appl. Phys. **107**, 09D918 (2010).
[4]C. M. Leung *et al.*, Rev. Sci. Instrum. **82**, 013903 (2011).
[5]S. W. Or and G. P. Carman, IEEE Trans. Magn. **41**, 2790 (2005).
[6]Y. M. Jia *et al.*, Adv. Mater. **20**, 4776 (2008).
[7]R. F. Harrington, *Introduction to Electromagnetic Engineering* (Dover Publications, NY, 2003).
[8]G. Engdahl, *Magnetostrictive Materials Handbook* (Academic, NY, 2000).
[9]T. Ikeda, *Fundamentals of Piezoelectricity* (Oxford University Press, Oxford, 1990).
[10]S. Y. Zhang, Ph.D. dissertation (The Hong Kong Polytechnic University) (unpublished).
[11]E. M. Syed, F. P. Dawson, and E. S. Rogers, Proc.-IEEE 32nd Annual Power Electronics Specialists Conference, 1761 (2001).